FLWRS v12.3 — Field of Lumina: Warp-Resonated Symmetry

Expanded edition (mathematical and experimental program)

Anton Kleschev Alevtinowitch
Independent Cyber-Researcher
Fynjyk@gmail.com

August 21, 2025

Abstract

This manuscript presents FLWRS (Field of Lumina) version 12.3: a consolidated, mathematically rigorous and experimentally actionable formulation of the Lumina hypothesis. Lumina denotes a fractal substrate whose projection into observable physics is mediated by a weak, near-identity selection operator denoted Luminissance. The present document develops the foundational equations of motion (the FED), provides a functional-analytic framework for well-posedness, formalizes the Luminissance operator in spectral and projectional forms, and derives experimentally-testable consequences across optics, precision clocks, and neurophysiology. We state and prove core theorems on local existence and uniqueness, provide a spectral-response lemma that links the operator's spectral imaginary part to modal dissipation, and formulate precise falsification criteria with required sensitivity thresholds. An extended Appendix sketches complete proofs and provides numerical recipes for reproducible spectral solvers. This is the working manuscript for experimental design, theoretical development, and numerical reproducibility of FLWRS v12.3.

Keywords: Lumina, Luminissance, fractional Laplacian, spectral selector, well-posedness, inverse problem, falsification.

Contents

1 Introduction and motivation **5**
- 1.1 Philosophical and physical rationale . . . 5
- 1.2 Relation to prior work . . . 5

2 Notation and conventions **5**

3 Mathematical preliminaries **6**
- 3.1 Sobolev spaces and basic embeddings . . . 6
- 3.2 Definitions of the fractional Laplacian . . . 6
- 3.3 Nonlinear convolution operator . . . 6

4 Fundamental Equation of Dynamics (FED) **7**

5 Modeling Luminissance: two paradigms **7**
- 5.1 (A) Linear spectral selector . . . 7
- 5.2 (B) Nonlinear weak projector . . . 7

6 Assumptions and hypotheses for theorems **8**

7 Main results (statements) **8**

8 Sketches of proofs and discussion **9**
- 8.1 Proof sketch for Theorem 7.1 . . . 9
- 8.2 Sketch for Lemma 7.2 . . . 9

9 Analytical tools and key inequalities **9**

10 Proof of local well-posedness (Theorem 7.1) **10**
- 10.1 Rewriting FED as integral equation . . . 10
- 10.2 Local Lipschitz estimates . . . 10
- 10.3 Contraction mapping argument . . . 11
- 10.4 Continuous dependence and uniqueness . . . 11

11 Energy estimates and continuation criteria **11**

12 Refinements: weaker regularity via fractional product tools **12**

13 Spectral preliminaries and operator properties **12**
- 13.1 Spectral multiplier operators . . . 12
- 13.2 Decomposition of σ into Hermitian/anti-Hermitian parts . . . 13

14 Derivation of modal evolution: rigorous form of Lemma 7.2 **13**
- 14.1 Equation in modal coordinates . . . 13
- 14.2 Evolution of modal power . . . 13
- 14.3 Remainder estimates . . . 13

15 Refined spectral analysis and resonance theory **14**
15.1 Linearized dispersion and growth rates . . . 14
15.2 Perturbation theory for near-resonant interactions . . . 14
15.3 Spectral filters: design and sensitivity . . . 15

16 Inverse problem: parameter estimation and adjoint-based gradient **15**
16.1 Cost functional and regularization . . . 15
16.2 Adjoint-state derivation (continuous) . . . 15
16.3 Adjoint PDE for FED (explicit form) . . . 16
16.4 Discrete adjoint and gradient computation (algorithm) . . . 16
16.5 Practical remarks . . . 17

17 Identifiability and Fisher information **17**
17.1 Linearized forward map and sensitivity matrix . . . 17
17.2 Fisher information matrix (FIM) . . . 18
17.3 Practical identifiability diagnostics . . . 18

18 Numerical methods: spectral discretization and time-stepping **18**
18.1 Spatial discretization: Fourier spectral method (periodic domain) . . . 18
18.2 Time-stepping schemes . . . 19
18.3 Computing fractional Laplacian . . . 19
18.4 Dealiasing and stability . . . 19
18.5 Algorithm: spectral forward solver (pseudocode) . . . 19
18.6 Parameter estimation loop (practical) . . . 20
18.7 Regularization strategies . . . 20

19 Validation, synthetic experiments and uncertainty quantification **20**
19.1 Synthetic data pipeline . . . 20
19.2 Bootstrap and ensemble methods . . . 21
19.3 Sensitivity analysis . . . 21

20 Practical implementation notes and software engineering **21**
20.1 Code structure suggestions . . . 21
20.2 Performance and parallelization . . . 21

21 Experimental design: principles and decision rules **21**
21.1 General experimental principles . . . 21
21.2 Decision rules (statistical thresholds) . . . 22

22 Falsification table and experimental "cheat-sheets" **22**
22.1 Table: Observables, signatures, decision rule . . . 22
22.2 Cheat-sheet: optics / resonator experiments . . . 23
22.3 Cheat-sheet: atomic clocks / precision timing . . . 23
22.4 Cheat-sheet: interferometry / gravitational wave style detectors . . . 24
22.5 Cheat-sheet: EEG / neurophysiology . . . 24

23 Instrument sensitivity reference tables **25**
23.1 Table A: Optical resonator target sensitivities . . . 25
23.2 Table B: Atomic clock benchmarks . . . 25
23.3 Table C: EEG experiment benchmarks . . . 25

24 Reproducible notebook and computational environment **26**
24.1 Environment specification (conda) 26
24.2 requirements.txt (pip minimal) 27
24.3 Dockerfile (skeleton) 27
24.4 Notebook checklist and tests 27

25 Data management and experiment reproducibility **28**

A Appendix A: Full proof of local well-posedness and continuation **28**
A.1 Functional setting and assumptions 28
A.2 Fixed point map and bounds 28
A.3 A priori estimates and extension 29

B Appendix B: Full proof of spectral response lemma **29**

C Appendix C: Discrete adjoint derivations and verification **30**
C.1 Time-splitting operator Jacobians 30
C.2 Finite-difference check 30

D Appendix D: Numerical examples **30**

E Appendix E: Recommended checklist for experimental pre-registration **32**

F Acknowledgements **32**

G Bibliography **32**

1 Introduction and motivation

FLWRS (Field of Lumina) proposes that what we perceive as physical phenomena arise as projections of a deeper, fractal substrate, termed *Lumina*. Rather than a separate metaphysical claim, FLWRS is a formal program: (i) provide a precise dynamical equation coupling observable fields to Lumina through a weak operator (Luminissance); (ii) make mathematically rigorous claims on the existence and stability of dynamics; and (iii) derive concrete experimental signatures and falsification criteria accessible to modern instrumentation.

This introduction summarizes the conceptual motivation, situates the theory with respect to prior models (fractional dynamics, nonlocal operators, and weak-selection frameworks), and outlines the plan of the paper.

1.1 Philosophical and physical rationale

Lumina is postulated as a fractal, information-bearing substrate that itself remains unperturbed — an axiom we refer to as *Unstained Alaya*. The observable world corresponds to a projection of Lumina via a channel whose local fractal properties are encoded by a scalar field $d_{\mathrm{loc}}(x)$. The Luminissance operator implements a mild, structured selection in mode space, favoring or suppressing certain resonances. Physically, this formalism models subtle, nonlocal corrections to dynamics (for example, tiny spectral redistributions) that would be invisible in classical, short-range theories but detectable by sufficiently sensitive spectral and temporal measurements.

1.2 Relation to prior work

FLWRS synthesizes several threads:

- Fractional Laplacian and anomalous transport literature (Mathematical PDE community).
- Nonlocal nonlinear Schrödinger-type models in condensed matter and optics (physics).
- Weak selection and projectional models in information-processing theories.

The new emphasis is on a formally small but structured operator ($\mathcal{L}_{\mathrm{Luminissance}}$), paired with precise falsification conditions and reproducible numerical benchmarks.

2 Notation and conventions

Below we list conventions used throughout.

- Domain: $\Omega \subset \mathbb{R}^d$, either the periodic torus $\mathbb{T}^d$ (preferred for spectral computations) or $\mathbb{R}^d$ with decay/weighted spaces.
- Sobolev spaces: $H^s(\Omega)$ denotes the standard L^2-based Sobolev space of order s; $\|\cdot\|_{H^s}$ the corresponding norm.
- Fractional Laplacian: $(-\Delta)^{\alpha/2}$ denotes the fractional operator defined spectrally on the torus or via the principal-value integral in $\mathbb{R}^d$; we fix $\alpha \in (1, 2]$ unless stated otherwise.

- Fourier transform conventions: On the periodic domain we denote Fourier coefficients by $\widehat{f}(k)$ with $k \in \mathbb{Z}^d$ and use the standard normalization consistent with Parseval's identity.
- Spectral notation for modes: k denotes wave numbers; $P(k,t) := |\widehat{\psi}(k,t)|^2$.
- Operator notation: $\mathcal{L}_{\text{Luminissance}}$ denotes the Luminissance operator. Boldface symbols indicate vectors when necessary.

3 Mathematical preliminaries

We collect essential definitions and basic facts used in proofs.

3.1 Sobolev spaces and basic embeddings

For $s \geq 0$, $H^s(\Omega)$ denotes the Sobolev space, with equivalence to decay of Fourier coefficients on the torus. Classical embedding and interpolation inequalities are used without comment; refer to standard texts for proofs.

3.2 Definitions of the fractional Laplacian

We use the following definitions where convenient:

1. **Spectral definition (compact domain / torus).** If $-\Delta$ has eigenbasis $\{\phi_k\}$ with eigenvalues $\lambda_k \geq 0$, then $(-\Delta)^{\alpha/2} f = \sum_k \lambda_k^{\alpha/2} \langle f, \phi_k \rangle \phi_k$.
2. **Integral definition (Euclidean domain).** For sufficiently smooth f,

$$(-\Delta)^{\alpha/2} f(x) = C_{d,\alpha}\, \mathrm{PV} \int_{\mathbb{R}^d} \frac{f(x) - f(y)}{|x-y|^{d+\alpha}}\, dy,$$

   where PV indicates the principal value and $C_{d,\alpha}$ is a normalization constant.

Both definitions coincide for appropriate function classes and serve different purposes: spectral for numerical implementation and integral for certain estimates.

3.3 Nonlinear convolution operator

Given $K \in L^1(\Omega)$ symmetric, define

$$(K * |\psi|^2)(x) \;=\; \int_\Omega K(x-y)\, |\psi(y)|^2\, dy.$$

Standard Young's-convolution and product estimates apply.

4 Fundamental Equation of Dynamics (FED)

We take the FED to be the primary dynamical statement of FLWRS v12.3.

Definition 4.1 (Fundamental Equation of Dynamics (FED))**.** *Given* $\alpha \in (1, 2]$*,* $\psi : \mathbb{R} \times \Omega \to \mathbb{C}$ *satisfies*

$$i\partial_t \psi(t,x) \;=\; \Big[(-\Delta)^{\alpha/2} + V(x) + (K * |\psi|^2)(x) \Big] \psi(t,x) \;+\; \lambda\, \mathcal{L}_{\text{Luminissance}}[\psi](t,x),$$

where $V \in L^\infty(\Omega)$ *is the external potential,* $K \in L^1(\Omega)$ *the symmetric nonlinear kernel,* $\lambda \in \mathbb{R}$ *is a small scalar parameter, and* $\mathcal{L}_{\text{Luminissance}} : H^\alpha(\Omega) \to H^\alpha(\Omega)$ *is the Luminissance operator.*

Remark 4.2. *The form conserves the classical structure of a dispersive nonlinear system (modulo the* $\mathcal{L}_{\text{Luminissance}}$ *term). When* $\mathcal{L}_{\text{Luminissance}}$ *is skew-self-adjoint (purely anti-Hermitian) and* λ *real, the dynamics preserve the* L^2 *norm. However, generically* $\mathcal{L}_{\text{Luminissance}}$ *may have a small symmetric (dissipative) part, which introduces controlled dissipation described below.*

5 Modeling Luminissance: two paradigms

We make explicit two modeling paradigms for $\mathcal{L}_{\text{Luminissance}}$ that will be used throughout the manuscript: (A) a linear spectral selector and (B) a nonlinear weak projector. Both are near-identity in operator norm.

5.1 (A) Linear spectral selector

In the spectral representation (if available),

$$\widehat{\mathcal{L}_{\text{Luminissance}}[\psi]}(k) \;=\; \sigma(k)\, \widehat{\psi}(k),$$

with the canonical parameterization (chosen throughout)

$$\sigma(k) \;=\; 1 - \varepsilon\, s(k) + i\, \eta(k), \qquad \varepsilon \geq 0,\; s(k) \geq 0,\; \eta(k) \in \mathbb{R},$$

and with ε, η small in appropriate norms (e.g. $\sup_k |\varepsilon s(k)| \ll 1$, $\sup_k |\eta(k)| \ll 1$). The real part controls amplitude selection (through rescaling), while the imaginary part controls modal dissipation or gain.

5.2 (B) Nonlinear weak projector

An alternative is to write

$$\mathcal{L}_{\text{Luminissance}}[\psi] \;=\; -\gamma\, (I - P_\phi)\psi + N[\psi],$$

where P_ϕ is projection onto one or several resonance modes ϕ (which may depend slowly on ψ), $\gamma > 0$ is a small damping coefficient, and $N[\psi] = O(\|\psi\|_{H^\alpha}^p)$ is a higher-order nonlinear correction.

6 Assumptions and hypotheses for theorems

We collect the working hypotheses used in the main theorems.

Assumption 6.1 (Spaces and operators)**.** *Fix $\alpha \in (1, 2]$. Assume*

(a) $\psi_0 \in H^\alpha(\Omega)$.

(b) $V \in L^\infty(\Omega)$ *(for more regularity one may assume C^∞).*

(c) $K \in L^1(\Omega)$ *and symmetric:* $K(x) = K(-x)$.

(d) The operator $\mathcal{L}_{\text{Luminissance}} : H^\alpha \to H^\alpha$ *is bounded with* $\|\mathcal{L}_{\text{Luminissance}}\|_{H^\alpha \to H^\alpha} \leq C_{\mathcal{L}_{\text{Luminissance}}}$.

(e) The parameter λ *satisfies* $|\lambda|\, C_{\mathcal{L}_{\text{Luminissance}}} \ll 1$ *(quantitative smallness).*

Remark 6.2. *Assumption (d) may be verified in particular when* $\mathcal{L}_{\text{Luminissance}}$ *is given by a spectral multiplier* $\sigma(k)$ *with* $|\sigma(k) - 1| \leq \delta \ll 1$ *uniformly.*

7 Main results (statements)

We state two principal results: local well-posedness (existence and uniqueness) and the spectral-response lemma linking $\operatorname{Im}\sigma$ to modal dissipation.

Theorem 7.1 (Local well-posedness in H^α)**.** *Under Assumption 6.1, for any initial datum $\psi_0 \in H^\alpha(\Omega)$ there exists $T > 0$ and a unique solution*

$$\psi \in C\Big([0, T]; H^\alpha(\Omega)\Big)$$

to the FED. The solution depends continuously on the initial datum in the H^α topology. Moreover, if in addition a-priori energy bounds hold (e.g., smallness conditions or dissipative control from $\mathcal{L}_{\text{Luminissance}}$), the solution extends globally in time.

Lemma 7.2 (Spectral response and linear modal dissipation)**.** *Assume the spectral representation from Section 5(A), with $\sigma(k) = 1 - \varepsilon s(k) + i\eta(k)$ and small parameters as above. Let $P(k, t) = |\widehat{\psi}(k, t)|^2$. Then, for small λ and at the level of linear response, the modal power evolution satisfies*

$$\partial_t P(k, t) \;=\; -2\lambda\, \operatorname{Im}\sigma(k)\, P(k, t) \;+\; R(k, t),$$

where the remainder $R(k, t)$ collects nonlinear transfer terms and contributions of order $O(\lambda\varepsilon, \lambda\eta^2)$.

Proposition 7.3 (Proxy clarity metric)**.** *Define a proxy metric for clarity as*

$$\mathcal{C}(d_{\text{loc}}) \;=\; \exp\Big(-\kappa\, |d_{\text{loc}} - 2|\Big), \qquad \kappa > 0.$$

Then $\mathcal{C}$ achieves its maximum 1 at $d_{\text{loc}} = 2$ and decays exponentially with deviation from 2. This function serves as a practical measure for experimental correlation to subjective clarity proxies.

8 Sketches of proofs and discussion

We outline the key ideas; full proofs appear in Part II and the Appendix.

8.1 Proof sketch for Theorem 7.1

Rewrite FED as an abstract ODE in H^α,

$$\partial_t \psi = -iA\psi + F(\psi),$$

with $A = (-\Delta)^{\alpha/2} + V$ and $F(\psi) = -i(K * |\psi|^2)\psi - i\lambda \mathcal{L}_{\text{Luminissance}}[\psi]$.

- Use properties of A (self-adjointness and generation of the group e^{-iAt}) to write a variation-of-constants formula.
- Show F is locally Lipschitz on bounded subsets of H^α: the convolution term is controlled using Young and algebra properties for Sobolev spaces with $\alpha > d/2$ or via fractional product rules for the general case.
- Apply a fixed-point (Picard) argument on $C([0,T]; H^\alpha)$ to obtain local existence; uniqueness follows from contraction estimates.
- Continuation criteria rely on a priori control of $\|\psi\|_{H^\alpha}$ which can be obtained from energy-like functionals and Gronwall inequalities, taking into account smallness of λ.

8.2 Sketch for Lemma 7.2

Projected to the spectral modes, the linear part contributes pure phase evolution and $\mathcal{L}_{\text{Luminissance}}$ contributes a small multiplicative perturbation $\sigma(k)$. From the mode equation for $\widehat{\psi}(k,t)$, compute $\partial_t P$ and isolate the non-Hermitian component coming from $\operatorname{Im}\sigma(k)$; the nonlinear transfers appear as convolution source terms and are collected in $R(k,t)$. This yields the displayed relation and the interpretation in terms of modal damping/amplification.

9 Analytical tools and key inequalities

We gather core analytic inequalities used repeatedly in proofs. Proofs of standard facts are omitted; references include Adams & Fournier, Grafakos, and standard PDE texts.

Lemma 9.1 (Young convolution inequality)**.** *Let $1 \le p, q, r \le \infty$ with $\frac{1}{p} + \frac{1}{q} = 1 + \frac{1}{r}$. If $f \in L^p$, $g \in L^q$ then $f * g \in L^r$ and $\|f * g\|_{L^r} \le \|f\|_{L^p} \|g\|_{L^q}$.*

Lemma 9.2 (Fractional product estimate)**.** *Let $s \ge 0$ and assume $s > \frac{d}{2}$ (so H^s is an algebra). Then for $u, v \in H^s(\Omega)$ there exists $C(s,d)$ such that*

$$\|uv\|_{H^s} \le C \|u\|_{H^s} \|v\|_{H^s}.$$

More generally, fractional Leibniz/product rules hold (Kato–Ponce-type)

$$\|D^s(uv)\|_{L^2} \le C\Big(\|u\|_{H^s}\|v\|_{L^\infty} + \|u\|_{L^\infty}\|v\|_{H^s}\Big).$$

Lemma 9.3 (Convolution in Sobolev spaces)**.** *Let $K \in L^1(\Omega)$ and $f \in H^s(\Omega)$, then $K * f \in H^s(\Omega)$ and $\|K * f\|_{H^s} \le \|K\|_{L^1}\|f\|_{H^s}$.*

Remark 9.4. *When $\alpha \le d/2$ the algebra property of H^α may fail; in that regime one needs more careful product estimates (e.g. using Besov spaces or Bony paraproduct). For simplicity we present the well-posedness argument in a range where standard Sobolev algebra rules apply or else outline how to adapt the argument using fractional product machinery.*

10 Proof of local well-posedness (Theorem 7.1)

This section gives a complete proof of Theorem 7.1 stated in Part I. We follow a classical Picard fixed-point strategy in $C([0,T];H^\alpha)$.

10.1 Rewriting FED as integral equation

Let $A := (-\Delta)^{\alpha/2} + V(x)$ (with domain H^α). Under our assumptions A generates a unitary group $U(t) = e^{-iAt}$ on L^2 and on H^α (by spectral calculus). The FED is equivalent to the Duhamel integral equation

$$\psi(t) \;=\; U(t)\psi_0 - i\int_0^t U(t-s)\Big[(K * |\psi(s)|^2)\psi(s) + \lambda\mathcal{L}_{\text{Luminissance}}[\psi(s)]\Big]\,ds.$$

Define the nonlinear mapping $\mathcal{T}$ on a Banach space $X_T := C([0,T];H^\alpha)$ by

$$\mathcal{T}[\phi](t) \;=\; U(t)\psi_0 - i\int_0^t U(t-s)\Big[(K * |\phi(s)|^2)\phi(s) + \lambda\mathcal{L}_{\text{Luminissance}}[\phi(s)]\Big]\,ds.$$

10.2 Local Lipschitz estimates

We will show that $\mathcal{T}$ maps the closed ball $B_R := \{\phi \in X_T : \sup_{t\in[0,T]}\|\phi(t)\|_{H^\alpha} \le R\}$ into itself and is a contraction for sufficiently small T.

Lemma 10.1 (Nonlinear estimate)**.** *Assume $K \in L^1(\Omega)$, $\mathcal{L}_{\text{Luminissance}}$ bounded on H^α, and α large enough that H^α is an algebra (or use fractional-product rules instead). Fix $R > 0$. Then there exists $C_R > 0$ such that for any $\phi, \tilde\phi \in B_R$ and $t \in [0,T]$,*

$$\Big\|(K * |\phi|^2)\phi - (K * |\tilde\phi|^2)\tilde\phi\Big\|_{H^\alpha} \le C_R\,\|\phi - \tilde\phi\|_{H^\alpha}.$$

Proof. Write

$$(K * |\phi|^2)\phi - (K * |\tilde\phi|^2)\tilde\phi = (K * (|\phi|^2 - |\tilde\phi|^2))\phi + (K * |\tilde\phi|^2)(\phi - \tilde\phi).$$

Using the convolution estimate and product rule, and the algebra property of H^α,

$$\begin{aligned}\|(K * (|\phi|^2 - |\tilde\phi|^2))\phi\|_{H^\alpha} &\le \|K\|_{L^1}\||\phi|^2 - |\tilde\phi|^2\|_{H^\alpha}\|\phi\|_{H^\alpha}\\ &\le C\|K\|_{L^1}(\|\phi\|_{H^\alpha} + \|\tilde\phi\|_{H^\alpha})\|\phi - \tilde\phi\|_{H^\alpha}\|\phi\|_{H^\alpha}.\end{aligned}$$

Similarly,

$$\|(K * |\tilde\phi|^2)(\phi - \tilde\phi)\|_{H^\alpha} \le \|K\|_{L^1}\|\tilde\phi\|_{H^\alpha}^2\|\phi - \tilde\phi\|_{H^\alpha}.$$

Combining and absorbing constants gives the desired Lipschitz estimate with C_R depending on R and $\|K\|_{L^1}$. □

Lemma 10.2 (Luminissance Lipschitz)**.** *If $\mathcal{L}_{\text{Luminissance}}$ is bounded on H^α with operator norm $C_{\mathcal{L}_{\text{Luminissance}}}$, then*

$$\|\mathcal{L}_{\text{Luminissance}}[\phi] - \mathcal{L}_{\text{Luminissance}}[\tilde{\phi}]\|_{H^\alpha} \le C_{\mathcal{L}_{\text{Luminissance}}} \|\phi - \tilde{\phi}\|_{H^\alpha}.$$

Proof. This is immediate from linearity and boundedness (or from a nonlinear bound if $\mathcal{L}_{\text{Luminissance}}$ has small nonlinear part; one replaces $C_{\mathcal{L}_{\text{Luminissance}}}$ by a local Lipschitz constant). □

10.3 Contraction mapping argument

For $\phi, \tilde{\phi} \in B_R$,

$$\begin{aligned}\|\mathcal{T}[\phi](t) - \mathcal{T}[\tilde{\phi}](t)\|_{H^\alpha} &\le \int_0^t \left\| (K * |\phi|^2)\phi - (K * |\tilde{\phi}|^2)\tilde{\phi} \right\|_{H^\alpha} ds + |\lambda| \int_0^t \|\mathcal{L}_{\text{Luminissance}}[\phi] - \mathcal{L}_{\text{Luminissance}}[\tilde{\phi}]\| \\ &\le (C_R + |\lambda| C_{\mathcal{L}_{\text{Luminissance}}}) \int_0^t \|\phi(s) - \tilde{\phi}(s)\|_{H^\alpha}\, ds.\end{aligned}$$

Taking supremum in $t \in [0, T]$ yields

$$\|\mathcal{T}[\phi] - \mathcal{T}[\tilde{\phi}]\|_{X_T} \le (C_R + |\lambda| C_{\mathcal{L}_{\text{Luminissance}}}) T \|\phi - \tilde{\phi}\|_{X_T}.$$

Choose T so small that $(C_R + |\lambda| C_{\mathcal{L}_{\text{Luminissance}}})T < 1/2$ (for example). Then $\mathcal{T}$ is a contraction on B_R.

Similarly, for mapping into B_R, we estimate $\|\mathcal{T}[\phi]\|_{X_T}$ using

$$\|\mathcal{T}[\phi]\|_{X_T} \le \|\psi_0\|_{H^\alpha} + T(C'_R + |\lambda| C_{\mathcal{L}_{\text{Luminissance}}})(1 + R^3),$$

and choose R large enough and then T small so that the right-hand side is $\le R$. Hence $\mathcal{T}$ maps B_R into itself.

By Banach fixed point theorem we obtain a unique fixed point in B_R, i.e. a unique solution $\psi \in X_T$.

10.4 Continuous dependence and uniqueness

Uniqueness is obvious from the contraction estimate. Continuous dependence on initial data follows by comparing solutions via the Duhamel formula and Gronwall-type estimates: if $\psi^{(1)}$, $\psi^{(2)}$ are solutions with initial data $\psi_0^{(1)}$ and $\psi_0^{(2)}$, then

$$\|\psi^{(1)}(t) - \psi^{(2)}(t)\|_{H^\alpha} \le \|\psi_0^{(1)} - \psi_0^{(2)}\|_{H^\alpha} + (C_R + |\lambda| C_{\mathcal{L}_{\text{Luminissance}}}) \int_0^t \|\psi^{(1)}(s) - \psi^{(2)}(s)\|_{H^\alpha}\, ds,$$

and Gronwall's lemma yields the continuous dependence.

□

11 Energy estimates and continuation criteria

To extend local solutions we derive energy-like bounds. Consider the (formal) energy functional

$$E[\psi] \;=\; \frac{1}{2}\langle \psi, (-\Delta)^{\alpha/2}\psi\rangle + \frac{1}{2}\langle \psi, V\psi\rangle + \frac{1}{4}\iint K(x-y)|\psi(x)|^2|\psi(y)|^2\, dxdy.$$

When $\mathcal{L}_{\text{Luminissance}}$ is skew-adjoint (purely imaginary multiplier with $\operatorname{Im}\sigma = 0$) and λ real, $E[\psi]$ is conserved. In the general case, we obtain differential inequalities.

Proposition 11.1 (A-priori energy inequality)**.** *Let $\psi(t)$ be a sufficiently smooth solution to FED. Then*

$$\frac{d}{dt}E[\psi(t)] \;=\; \mathrm{Re}\langle \partial_t\psi, \delta E/\delta\overline{\psi}\rangle \;=\; -\lambda\,\mathrm{Im}\langle \mathcal{L}_{\text{Luminissance}}[\psi], \delta E/\delta\overline{\psi}\rangle,$$

and in particular

$$\left|\frac{d}{dt}E[\psi(t)]\right| \le C|\lambda|\,\|\mathcal{L}_{\text{Luminissance}}[\psi]\|_{H^\alpha}\,\|\psi\|_{H^\alpha}.$$

Sketch. Differentiate $E[\psi(t)]$ using the chain rule and substitute $\partial_t\psi$ from FED. The linear dispersive part yields purely imaginary inner products which cancel in the real part. The contribution of $\mathcal{L}_{\text{Luminissance}}$ yields the displayed term. The inequality follows by Cauchy–Schwarz and boundedness of $\mathcal{L}_{\text{Luminissance}}$. □

Corollary 11.2 (Continuation criterion)**.** *If a solution $\psi(t)$ exists on $[0,T^*)$ with maximal $T^*<\infty$ and if there exists M such that $\sup_{t\in[0,T^*)}\|\psi(t)\|_{H^\alpha}\le M$, then the solution can be extended beyond T^* (i.e. blowup in finite time can only occur if $\|\psi\|_{H^\alpha}\to\infty$).*

Proof. Standard: the local well-posedness time T depends only on the bound of the H^α norm and parameters. If $\|\psi\|_{H^\alpha}$ remains bounded, one can restart the Picard iteration at $T^*-\delta$ and extend. □

12 Refinements: weaker regularity via fractional product tools

When α does not guarantee the algebra property ($\alpha\le d/2$), we replace naive product estimates with fractional product/commutator estimates. A standard Kato–Ponce or Coifman–Meyer paraproduct decomposition yields boundedness of the mapping $\phi\mapsto(K*|\phi|^2)\phi$ from H^α to itself under milder conditions (for example, when $\alpha>(d/2)-\delta$ with additional Besov control). The technical machinery is standard in the PDE literature; we only remark that this uses paraproducts and Bony decomposition, and the argument modifies the Lipschitz constant accordingly.

13 Spectral preliminaries and operator properties

We now prepare tools to analyze $\mathcal{L}_{\text{Luminissance}}$ in spectral representation and to derive the modal response formula.

13.1 Spectral multiplier operators

Let $\{e_k\}$ be an orthonormal eigenbasis of $(-\Delta)^{\alpha/2}+V$ on the torus, with eigenvalues $\omega_k\ge 0$ (ordered). A spectral multiplier operator T_σ acts as $\widehat{T_\sigma f}(k)=\sigma(k)\widehat{f}(k)$. If $\sup_k|\sigma(k)|\le 1+\delta$, T_σ is bounded on H^s with norm $\le 1+\delta$ for any s.

Definition 13.1 (Near-identity spectral multiplier)**.** *A spectral multiplier $\sigma(k)$ is* near-identity *if $\sup_k|\sigma(k)-1|\le\delta\ll 1$. For such σ the induced operator $T_\sigma-I$ has small operator norm on H^s (bounded by $C\delta$).*

13.2 Decomposition of σ into Hermitian/anti-Hermitian parts

Write $\sigma(k) = \operatorname{Re}\sigma(k) + i\,\operatorname{Im}\sigma(k)$. The Hermitian (self-adjoint) part corresponds to $\operatorname{Re}\sigma$ and controls amplitude scaling; the anti-Hermitian part corresponds to $\operatorname{Im}\sigma$ and yields modal damping/gain.

Lemma 13.2 (Spectral operator bounds)**.** *If* $\sup_k |\sigma(k) - 1| \le \delta$*, then* $\|T_\sigma - I\|_{H^s \to H^s} \le C_s\delta$*. If moreover* $\sup_k |\operatorname{Im}\sigma(k)| \le \delta'$*, then* $\|\frac{1}{2}(T_\sigma - T_\sigma^*)\| \le C_s\delta'$ *and the dissipative part is controlled.*

14 Derivation of modal evolution: rigorous form of Lemma 7.2

We derive the modal equation more carefully, including remainder estimates.

14.1 Equation in modal coordinates

Let $\widehat{\psi}(k,t) = \langle \psi(t), e_k \rangle$. Projecting FED on e_k gives

$$i\partial_t \widehat{\psi}(k) = \omega_k \widehat{\psi}(k) + \widehat{\mathcal{N}[\psi]}(k) + \lambda\sigma(k)\widehat{\psi}(k),$$

where $\widehat{\mathcal{N}[\psi]}(k)$ denotes the modal transform of the nonlinear convolution term.

14.2 Evolution of modal power

Differentiate $P(k,t) = \widehat{\psi}(k)\overline{\widehat{\psi}(k)}$:

$$\partial_t P = \widehat{\psi}\overline{\partial_t \widehat{\psi}} + \overline{\widehat{\psi}}\partial_t \widehat{\psi}.$$

Substitute for $\partial_t\widehat{\psi}$ and its complex conjugate. The linear pure-phase term $i\omega_k$ cancels; the σ-term generates

$$\partial_t P\Big|_\sigma = i\lambda(\overline{\sigma(k)} - \sigma(k))P = -2\lambda\,\operatorname{Im}\sigma(k)\,P.$$

The nonlinear terms produce bilinear/trilinear convolution contributions which we group into $R(k,t)$.

14.3 Remainder estimates

Assume a bound $\|\psi(t)\|_{H^\alpha} \le M$ on the time interval of interest. Then using product and convolution inequalities,

$$|R(k,t)| \le C(M) \sum_{k_1,k_2} |\widehat{\psi}(k_1)|\,|\widehat{\psi}(k_2)|\,|\widehat{\psi}(k-k_1-k_2)|,$$

and $\|R(\cdot,t)\|_{\ell^1} \le C'(M)$, giving control on the aggregate nonlinear transfer. For linear-response we consider the regime where $\lambda \ll 1$ and initial amplitudes are small enough so that R is subleading.

15 Refined spectral analysis and resonance theory

This section develops a refined spectral viewpoint on the Luminissance operator, resonant amplification/suppression, and linear stability considerations. We retain the spectral multiplier parameterization

$$\sigma(k) = 1 - \varepsilon s(k) + i\,\eta(k),$$

with smallness assumptions $\sup_k |\varepsilon s(k)| \ll 1$ and $\sup_k |\eta(k)| \ll 1$.

15.1 Linearized dispersion and growth rates

Consider the linearized FED around a small-amplitude background (ignoring nonlinear convolution for the moment). For each mode k the linear equation reduces to

$$i\partial_t \widehat{\psi}(k) = \omega_k \widehat{\psi}(k) + \lambda\sigma(k)\widehat{\psi}(k),$$

i.e.

$$\partial_t \widehat{\psi}(k) = -i(\omega_k + \lambda \operatorname{Re}\sigma(k))\widehat{\psi}(k) - \lambda \operatorname{Im}\sigma(k)\widehat{\psi}(k).$$

Thus the modal amplitude evolves as

$$\widehat{\psi}(k,t) = \widehat{\psi}(k,0)\exp\Big(-i(\omega_k + \lambda \operatorname{Re}\sigma(k))t - \lambda \operatorname{Im}\sigma(k)\,t\Big).$$

Interpretation:

- $\omega_k + \lambda \operatorname{Re}\sigma(k)$ — frequency shift of mode k.
- $-\lambda \operatorname{Im}\sigma(k)$ — exponential damping (if > 0) or growth (if < 0) rate.

A mode k is *linearly unstable* if $\lambda \operatorname{Im}\sigma(k) < 0$ (negative damping, net gain). For typical physical modeling we expect $\lambda > 0$ and $\eta(k) = \operatorname{Im}\sigma(k) \geq 0$; in that case $\lambda\eta(k) > 0$ implies damping.

15.2 Perturbation theory for near-resonant interactions

When nonlinear coupling is present, resonant triads/quartets can mediate energy transfer between modes. Denote the three-wave interaction coefficient symbolically by $T(k; k_1, k_2)$ arising from the convolution kernel K. The resonance condition (for energy-conserving transfer) in the dispersive framework is

$$\omega_k \;=\; \omega_{k_1} + \omega_{k_2} \pmod{2\pi/T},$$

and near-resonances with mismatch $\Delta\omega := \omega_k - \omega_{k_1} - \omega_{k_2}$ lead to slow secular transfer on the timescale $|\Delta\omega|^{-1}$.

Perturbatively, one can derive amplitude equations for slowly varying envelopes $a_k(t)$ (multiple-scale expansion). To leading order one obtains

$$\dot{a}_k = -\lambda \operatorname{Im}\sigma(k) a_k + \sum_{k_1,k_2} \mathcal{M}_{k;k_1,k_2} a_{k_1} a_{k_2} e^{i\Delta\omega t} + \dots$$

Averaging over fast oscillations filters out non-resonant interactions; the remaining resonant set determines long-time energy redistribution. Luminissance, entering via the damping term, modulates the secular transfer by altering growth/decay rates and thus the effective resonance balance.

15.3 Spectral filters: design and sensitivity

In experiments one can attempt to engineer $s(k)$ to target specific k-bands. From the linear relation for modal power (Lemma 7.2), the *observable* relative change per unit time in $P(k)$ due to $\mathcal{L}_{\text{Luminissance}}$ is $\approx -2\lambda\eta(k)P(k)$; hence the sensitivity to $\eta(k)$ is proportional to $P(k)$. Design principles:

- maximize $P(k)$ in the target band (pump that mode) to amplify the signal;
- ensure narrow-band $s(k)$ to avoid smearing the effect across many modes;
- calibrate λ experimentally by applying controlled perturbations with known coupling.

16 Inverse problem: parameter estimation and adjoint-based gradient

The inverse problem is to estimate parameter vector θ (e.g. $\theta = (\alpha, \lambda, \varepsilon, \text{param}(s), \text{param}(\eta))$) from measurements. We denote the forward map by

$$\mathcal{F} : \theta \mapsto d_{\text{pred}} = \mathcal{M}(\psi(\theta)),$$

where $\psi(\theta)$ is the solution of FED for given θ and $\mathcal{M}$ is the measurement operator that maps the field to observables (examples: sampled spectral power at times, autocorrelation function, PLV).

16.1 Cost functional and regularization

Define the least-squares Tikhonov-regularized cost

$$\mathcal{J}(\theta) \;=\; \frac{1}{2}\|\mathcal{M}(\psi(\theta)) - d_{\text{obs}}\|^2_{\Sigma^{-1}} + \frac{\mu}{2}\|\mathcal{R}(\theta)\|^2,$$

where Σ is the data covariance (noise), $\|\cdot\|^2_{\Sigma^{-1}}$ denotes the Mahalanobis norm, $\mathcal{R}(\theta)$ is a regularizer (e.g. Tikhonov or Sobolev penalty), and $\mu > 0$ is the regularization weight.

To minimize $\mathcal{J}$ we need gradient information $\nabla_\theta \mathcal{J}$. Direct differentiation would require differentiating the PDE solver; instead we derive the adjoint-state equations.

16.2 Adjoint-state derivation (continuous)

Let $u = \psi(\theta)$ solve FED written abstractly as

$$\mathcal{G}(u, \theta) = 0,$$

where $\mathcal{G}(u, \theta) := i\partial_t u - \mathcal{A}(u, \theta)$ and $\mathcal{A}$ denotes the spatial operator in the right-hand side of FED (including nonlinearity and $\mathcal{L}_{\text{Luminissance}}$). Linearizing around u yields

$$D_u\mathcal{G}[\delta u] + D_\theta\mathcal{G}[\delta\theta] = 0.$$

For a scalar cost $\mathcal{J}(\theta) = \frac{1}{2}\|\mathcal{M}(u) - d_{\text{obs}}\|^2 + \frac{\mu}{2}\|\mathcal{R}(\theta)\|^2$, the directional derivative is

$$\delta\mathcal{J} = \langle \mathcal{M}(u) - d_{\text{obs}}, \mathcal{M}'(u)[\delta u]\rangle + \mu\langle \mathcal{R}(\theta), \mathcal{R}'(\theta)[\delta\theta]\rangle.$$

Introduce the adjoint variable $p(t,x)$ solving the adjoint PDE (backward in time) such that

$$\langle \mathcal{M}(u) - d_{\text{obs}}, \mathcal{M}'(u)[\delta u] \rangle = \langle p, D_u \mathcal{G}[\delta u] \rangle,$$

for all admissible δu, with appropriate terminal/boundary conditions. Then combining with the linearized PDE gives

$$\delta \mathcal{J} = -\langle p, D_\theta \mathcal{G}[\delta\theta] \rangle + \mu \langle \mathcal{R}(\theta), \mathcal{R}'(\theta)[\delta\theta] \rangle,$$

so the gradient is

$$\nabla_\theta \mathcal{J} \;=\; -D_\theta \mathcal{G}^*[p] + \mu \mathcal{R}'(\theta)^* \mathcal{R}(\theta).$$

16.3 Adjoint PDE for FED (explicit form)

For FED, $D_u \mathcal{G}$ is obtained by linearizing the right-hand side. Writing

$$i\partial_t \delta u = L_{\text{lin}}(t)[\delta u] + \lambda D_u \mathcal{L}_{\text{Luminissance}}[u][\delta u],$$

where $L_{\text{lin}}(t)$ is the linearized operator from $(-\Delta)^{\alpha/2} + V + (K * |\cdot|^2)\cdot$ and the linearization of the convolution term depends on $u(t)$. The adjoint PDE (formal) is

$$-i\partial_t p = L_{\text{lin}}(t)^* p + \lambda (D_u \mathcal{L}_{\text{Luminissance}}[u])^* p + \mathcal{M}'(u)^* (\mathcal{M}(u) - d_{\text{obs}}),$$

with terminal condition $p(T) = 0$ if the cost integrates mismatch over time, or $p(T) = \mathcal{M}'(u(T))^* (\mathcal{M}(u(T)) - d_{\text{obs}})$ for terminal-only measurements. See algorithm boxes below.

16.4 Discrete adjoint and gradient computation (algorithm)

On a discrete grid/time-stepping scheme the steps to compute $\nabla_\theta \mathcal{J}$ are:

1. Forward solve: integrate FED forward for given θ to obtain u^n for $n = 0..N$.
2. Compute data misfit $\delta d = \mathcal{M}(u) - d_{\text{obs}}$ and evaluate residual terms at measurement times.
3. Backward (adjoint) solve: integrate the discrete adjoint PDE backward using the transpose Jacobians of the time-stepping scheme; accumulate sensitivity terms $S_\theta = -\sum_n (D_\theta \mathcal{G}(u^n, \theta))^T p^n$.
4. Assemble gradient: $\nabla_\theta \mathcal{J} = S_\theta + \mu \mathcal{R}'(\theta)^T \mathcal{R}(\theta)$.

We provide pseudo-code for a typical time-splitting spectral solver + adjoint.

Algorithm 1: Forward + Adjoint gradient evaluation (schematic)

1. Input: θ, initial state u^0, measurement operator $\mathcal{M}$, data d_{obs}.
2. Forward:
   - for $n = 0..N-1$ do: $u^{n+1} = \textsc{TimeStep}(u^n, \theta)$ (store necessary intermediates).
3. Residual: compute $r^n = \mathcal{M}(u^n) - d^n_{\text{obs}}$ for measurement times.
4. Initialize adjoint $p^N = 0$ (or terminal residual if terminal cost).
5. Backward:
   - for $n = N-1..0$ do: $p^n = \textsc{AdjointStep}(p^{n+1}, u^n, \theta, r^n)$, accumulate sensitivity $S_\theta += -(D_\theta \textsc{TimeStep})(u^n, \theta)^T p^{n+1}$.
6. Output: gradient $\nabla_\theta \mathcal{J} = S_\theta + \mu \mathcal{R}'(\theta)^T \mathcal{R}(\theta)$.

16.5 Practical remarks

- Implementation requires storing or recomputing (via checkpointing) forward states to evaluate linearized step Jacobians in the adjoint.
- When $\mathcal{L}_{\text{Luminissance}}$ is spectral, $D_\theta \mathcal{L}_{\text{Luminissance}}$ is straightforward: e.g. derivatives w.r.t. ε or spectral shape parameters enter multiplicatively in Fourier space.
- Automatic differentiation frameworks can implement discrete adjoint for moderate problem sizes; for large PDEs custom adjoints are more efficient.

17 Identifiability and Fisher information

Understanding which parameters can be reliably estimated from given data requires analysis of the linearized forward operator around a nominal parameter θ_0.

17.1 Linearized forward map and sensitivity matrix

Linearize the forward map: for small perturbation $\delta\theta$,

$$\mathcal{F}(\theta_0 + \delta\theta) \approx \mathcal{F}(\theta_0) + \mathcal{J}_\theta \delta\theta,$$

where $\mathcal{J}_\theta$ is the (Fréchet) Jacobian of $\mathcal{F}$. For discrete observations (vector-valued data) this reduces to a matrix $J \in \mathbb{R}^{m \times p}$.

17.2 Fisher information matrix (FIM)

Assume additive Gaussian measurement noise with covariance Σ. The Fisher information matrix is

$$\mathcal{I}(\theta_0) = J^T \Sigma^{-1} J.$$

Interpretation:

- Large eigenvalues of $\mathcal{I}$ indicate directions in parameter space that are well-informed by the data.
- Small eigenvalues (near-zero) indicate non-identifiability or ill-conditioning.

Cramér–Rao lower bound: the covariance of any unbiased estimator $\hat{\theta}$ satisfies $\mathrm{Cov}(\hat{\theta}) \succeq \mathcal{I}(\theta_0)^{-1}$ (where inverse taken on the subspace of nonzero eigenvalues).

17.3 Practical identifiability diagnostics

- Compute singular value decomposition of J (or eigendecomposition of $\mathcal{I}$) to reveal identifiable subspace.
- Use active subspace or likelihood-informed subspace methods to reduce parameter dimension for inversion.
- Profile likelihoods: hold candidate parameters fixed and optimize others to compute marginal likelihood curves — practical for non-Gaussian posteriors.

18 Numerical methods: spectral discretization and time-stepping

This section gives practical numerical recipes for solving FED and for parameter estimation.

18.1 Spatial discretization: Fourier spectral method (periodic domain)

For $\Omega = [0, L]^d$ with periodic boundary conditions:

- Choose grid N^d equispaced points; represent $u(x)$ by its discrete Fourier transform $\hat{u}_k$.
- Fractional Laplacian applied spectrally: multiply each mode by $|k|^\alpha$ (with k scaled to $2\pi/L$).
- Nonlinear convolution $K * |u|^2$ computed in real space or via spectral multiplication of $\widehat{K}$ and discrete $|\widehat{u}|^2$.
- Apply dealiasing (2/3-rule) if necessary to control aliasing errors in nonlinear terms.

18.2 Time-stepping schemes

Given dispersive linear part and nonlinear term we recommend splitting or exponential integrators.

Strang splitting (linear / nonlinear split). For time step Δt:

$$u^{n+1} \approx e^{-i(\Delta t/2)L}\, \Phi_{\mathrm{NL}}^{\Delta t}\, e^{-i(\Delta t/2)L} u^n,$$

where $L = (-\Delta)^{\alpha/2} + V$ and $\Phi_{\mathrm{NL}}^{\Delta t}$ denotes flow of nonlinear ODE $\partial_t u = -i(K * |u|^2)u - i\lambda \mathcal{L}_{\mathrm{Luminissance}}[u]$ for time Δt (can be approximated by RK4 in real space).

Exponential Time Differencing (ETDRK4). When stiffness from high-frequency modes is severe, use ETDRK4 (Kassam & Trefethen):

$$u^{n+1} = e^{L\Delta t} u^n + (\text{quadrature of nonlinear terms with phi-functions}).$$

Implement carefully using precomputed phi-functions or contour integral approximations.

18.3 Computing fractional Laplacian

On the torus multiply $\widehat{u}_k$ by $(|k|^2)^{\alpha/2}$; if using physical units ensure correct 2π scaling:

$$k_{\mathrm{ang}} = \frac{2\pi}{L} k, \qquad \text{multiplier} = |k_{\mathrm{ang}}|^{\alpha}.$$

18.4 Dealiasing and stability

For quadratic/cubic nonlinearities use 2/3-rule: zero out modes with |k| > N/3 after multiplication in physical domain. Monitor conserved quantities in absence of $\mathcal{L}_{\mathrm{Luminissance}}$ to test implementation fidelity.

18.5 Algorithm: spectral forward solver (pseudocode)

```
Given: initial u0(x), parameters theta, N grid, dt, final time T
Precompute: grid, k-vectors, fractional multiplier M_k = |k_ang|^alpha
u = u0
for n in 0..(T/dt)-1:
  # Linear half step
  u_hat = fft(u)
  u_hat = exp(-i * dt/2 * M_k) * u_hat
  u = ifft(u_hat)
  # Nonlinear full step (in physical space)
  NL = compute_nonlinear(u, theta)   # returns -i[(K*|u|^2)u + lambda L[u]]
  u = u + dt * NL  # simple Euler or RK stage; prefer RK4
  # Linear half step
  u_hat = fft(u)
  u_hat = exp(-i * dt/2 * M_k) * u_hat
  u = ifft(u_hat)
end
```

18.6 Parameter estimation loop (practical)

Use gradient-based optimization with adjoint gradients (or derivative-free methods if adjoint unavailable).

1. Initialize $\theta^{(0)}$.
2. For iteration m:
   - Forward solve to get $u(\theta^{(m)})$ and compute cost $\mathcal{J}$.
   - Compute gradient $\nabla_\theta \mathcal{J}$ via adjoint (Algorithm above).
   - Update $\theta^{(m+1)} = \theta^{(m)} - \alpha_m H_m^{-1} \nabla_\theta \mathcal{J}$ (choose step size α_m and preconditioner / approximate Hessian H_m; use L-BFGS or Gauss-Newton).
   - Project parameters to feasible set (positivity of ε, η bounds).
3. Stopping: gradient norm small or relative decrease small.

18.7 Regularization strategies

Because inverse problems are often ill-posed:

- Use Tikhonov regularization $\|\theta - \theta_{\text{prior}}\|_W^2$ to incorporate prior knowledge.
- Use sparsity or smoothness priors for spectral shape parameters (penalize high-frequency roughness of $s(k)$, $\eta(k)$).
- Employ hierarchical Bayesian models for simultaneous noise and parameter estimation (EM or MCMC).

19 Validation, synthetic experiments and uncertainty quantification

Robust validation is crucial before experimental deployment. We outline a pipeline.

19.1 Synthetic data pipeline

1. Choose ground-truth θ_{true}.
2. Generate forward solution $u_{\text{true}}(t)$ via a high-fidelity solver (sufficient resolution).
3. Compute observables $d_{\text{true}} = \mathcal{M}(u_{\text{true}})$.
4. Add synthetic noise: $d_{\text{obs}} = d_{\text{true}} + \eta_{\text{noise}}$ (choose noise model: Gaussian additive, Poisson, or correlated noise with covariance Σ).
5. Use the inversion pipeline to estimate $\hat{\theta}$ from d_{obs}.
6. Evaluate metrics: parameter error $\|\hat{\theta} - \theta_{\text{true}}\|$, predictive misfit $\|\mathcal{F}(\hat{\theta}) - d_{\text{true}}\|$, profile likelihoods, and coverage of uncertainty quantification.

19.2 Bootstrap and ensemble methods

Use bootstrap-resampling of the synthetic noise to obtain empirical parameter distributions, or run MCMC (if computationally feasible) to sample the posterior distribution.

19.3 Sensitivity analysis

Compute sensitivity indices (Sobol' or derivative-based) to determine which parameters strongly influence observables; reduce estimation dimensionality accordingly.

20 Practical implementation notes and software engineering

20.1 Code structure suggestions

- Core modules: spectral solver (forward), adjoint solver, measurement operator, optimization/estimation module, utilities (IO, plotting).
- Use unit tests for the spectral derivative, fractional Laplacian, mass conservation (when $\lambda = 0$ and $\mathcal{L}_{\text{Luminissance}}$ skew-adjoint), and adjoint consistency (finite-difference check).
- Use checkpointing for adjoint to balance memory and recomputation (Revolve algorithm or simple periodic checkpointing).

20.2 Performance and parallelization

- FFT libraries (FFTW, MKL) for high-performance transforms.
- For multi-dimensional large grid runs, use MPI with slab or pencil domain decomposition.
- GPU acceleration for FFT+pointwise operations (cuFFT) when available.

21 Experimental design: principles and decision rules

This section translates the mathematical predictions into concrete experimental protocols and decision rules. We stress reproducibility, pre-registration of analysis pipelines, and clear acceptance/rejection thresholds.

21.1 General experimental principles

1. **Controlled excitation:** to maximize detectability of $\mathcal{L}_{\text{Luminissance}}$-effects, prepare systems with large modal power $P(k)$ in target bands (pump/drive).
2. **Differential protocol:** compare runs with nominally identical conditions except for a controlled tuning parameter expected to change coupling to Lumina (e.g. minor change in boundary conditions, phase of injected pump, or environment).

3. **Long baseline and replication:** record sufficiently long time series to resolve slow secular changes and perform replicated runs ($n \geq 5$–10).

4. **Blind analysis and pre-registration:** lock analysis pipeline before unblinding data.

5. **Noise characterization:** measure noise floor and temporal correlations to compute SNR and covariance matrix Σ for inverse problem.

21.2 Decision rules (statistical thresholds)

Adopt standard frequentist thresholds with pre-specified corrections for multiple tests:

- Single-test detection: require SNR ≥ 5 (corresponds roughly to p $\lesssim$ 3e-7 for Gaussian noise).
- Model comparison (power-law vs exponential tails): prefer more parsimonious model by AIC/BIC; require ΔAIC ≥ 10 or Akaike weight > 0.95 to claim preference.
- For parameter estimation: report 95% confidence intervals (via Fisher/approximate posterior or bootstrap).

22 Falsification table and experimental "cheat-sheets"

The following tables summarize observables, predicted signatures and the minimal instrument sensitivity required to test FLWRS in representative domains.

22.1 Table: Observables, signatures, decision rule

Observable	Predicted signature (FLWRS)	Required sensitivity	Decision rule
Spectral power in narrow mode k	Relative change $\Delta P_k/P_k \approx -2\lambda\eta(k)T_{\text{int}}$	Detect $\Delta P_k/P_k$ at SNR ≥ 5	If SNR < 5 for all $k \Rightarrow$ reject model parameters
Autocorrelation / coherence $C(t)$	Long-time tail: power-law decay $t^{-\beta(\alpha)}$ vs expo	Time-range spanning $\geq$ 1–2 decades, resolution to distinguish slopes	Compare fits; prefer power-law if ΔAIC ≥ 10
Phase-locking value (neuronal PLV)	Systematic decrease with $\lvert d_{\text{loc}} - 2\rvert$	PLV change resolvable with $p < 0.01$ ($n \geq 10$)	Reject if no stat. significant dependence

22.2 Cheat-sheet: optics / resonator experiments

Goal: detect small spectral redistribution in a high-Q optical resonator.

Setup suggestions

- High-finesse whispering-gallery or Fabry–Pérot cavity with tunable pump to selectively populate mode k_0.
- Heterodyne detection for amplitude and phase of modes; narrow-band filtering to isolate target bands.
- Environmental control: temperature stability $<$ mK, vibration isolation.

Parameter region to probe

- Integration time $T_{\text{int}} \sim$ seconds–minutes per run; replicate 10–20 runs.
- Target fractional sensitivity to mode power: $\delta P/P \lesssim 10^{-6}$ (optical shot-noise limited detectors may achieve this with averaging).
- Sweep narrow-band selector $s(k)$ by modulating cavity coupling or injecting tunable pump.

Analysis checklist

1. Calibrate detector linearity and dynamic range.
2. Estimate noise covariance Σ (including $1/f$ and colored noise).
3. Fit $\Delta P_k/P_k$ across runs and compute SNR and p-values (with multiple testing correction).

22.3 Cheat-sheet: atomic clocks / precision timing

Goal: test for tiny fractional frequency shifts or decoherence tails due to fractional transport.

Setup suggestions

- Optical lattice clocks or single-ion clocks with frequency stability $10^{-18}/\sqrt{\text{Hz}}$ or better.
- Ramsey/echo sequences to probe coherence and measure autocorrelation tails.
- Synchronized comparisons between two co-located or separated clocks to control systematics.

Parameter region

- Probe fractional frequency shift sensitivity at level $< 10^{-18}$ for integration times of thousands of seconds.
- Look for deviations from exponential coherence decay—compare residuals to power-law models.

Analysis

1. Ensure systematic corrections (blackbody, Zeeman, AC Stark).
2. Use Allan deviation and time-domain fits to identify non-exponential tails.
3. Use model selection (AIC/BIC) and bootstrap to estimate significance.

22.4 Cheat-sheet: interferometry / gravitational wave style detectors

Goal: analyze narrow-band mode power redistribution in high-finesse interferometers.

Setup suggestions

- Use auxiliary cavity modes or sideband pumping to create localized modal power.
- Balanced detection and common-mode rejection to reduce seismic and laser noise.

Parameter region

- Target relative power changes $\delta P/P \lesssim 10^{-8}$–$10^{-6}$ (depends on band and averaging).
- Time-domain correlation analysis for long tails or small drifts.

22.5 Cheat-sheet: EEG / neurophysiology

Goal: test link between local fractalization (d_{loc}) and phase-locking / clarity proxies.

Setup suggestions

- High-density EEG (64–256 channels) with high sample rate (≥ 1 kHz) for broadband analysis.
- Controlled manipulations that plausibly influence local fractality (sensory modulation, pharmacological, or transcranial stimulation).
- Careful artifact rejection (blink, muscle, line noise).

Parameter region and metrics

- Estimate local spectral slopes in sliding windows to compute d_{loc}.
- Compute PLV, phase entropy and compare across experimental conditions.
- Require replication across subjects ($n \geq 10$) and within-subject repeated trials (≥ 20).

Analysis checklist

1. Pre-register hypotheses (which bands, electrodes, and time windows).
2. Use nonparametric cluster-based statistics to control multiple comparisons.
3. Report effect sizes and corrected p-values; perform power analysis in advance.

23 Instrument sensitivity reference tables

Below we provide rough sensitivity levels and recommended experimental standards. These are illustrative and must be adapted to actual lab specs.

23.1 Table A: Optical resonator target sensitivities

Instrument / Parameter	Typical reachable sensitivity	N
Photodetector (shot-noise limited)	$\delta P/P \sim 10^{-8}$ – 10^{-6}	with averaging and high optical p
Heterodyne phase noise floor	$\sim 10^{-6}$ rad	depends on local oscillator stal
Cavity frequency stability	fractional $\sim 10^{-15}$ – 10^{-17}	modern ultra-stable cav

23.2 Table B: Atomic clock benchmarks

Clock type	Typical stability	Not
Single-ion optical clock	$\sigma_y(\tau) \sim 10^{-18}$ at 10^4 s	Best laboratori
Optical lattice clock	$\sigma_y(\tau) \sim 10^{-18}$	Large ensembles can he
Coherence measurement resolution	time-domain tail sensitivity	depends on Ramsey/echo sequenc

23.3 Table C: EEG experiment benchmarks

Metric	Target precision	Notes
PLV change detectability	ΔPLV $\gtrsim 0.02$ – 0.05	depends on trial count and SNR
Spectral slope estimation	slope error $\lesssim 0.05$	using wavelet or multitaper methods
Sampling rate	≥ 1 kHz	recommended for broadband effects

24 Reproducible notebook and computational environment

This section provides a reproducible notebook plan, environment specification, and instructions for running the spectral demos and parameter sweeps.

```
FLWRS_v123/
|-- README.md
|-- environment.yml        # conda environment specification
|-- requirements.txt       # pip requirements
|-- notebooks/
|   |-- spectral_demo.ipynb
|   |-- parameter_sweep.ipynb
|   |-- adjoint_tutorial.ipynb
|-- src/
|   |-- forward_solver.py
|   |-- adjoint_solver.py
|   |-- inversion.py
|   |-- utils.py
|-- data/
|   |-- synthetic/
|-- tests/
|   |-- test_mass_conservation.py
|-- docker/
    |-- Dockerfile
    |-- entrypoint.sh
```

24.1 Environment specification (conda)

Provide both conda and pip specifications for portability.

```
name: flwrs123
channels:
  - conda-forge
dependencies:
  - python=3.10
  - numpy
  - scipy
  - matplotlib
  - jupyterlab
  - notebook
  - numba
  - fftw
  - h5py
  - pandas
  - scikit-learn
  - pyfftw
  - pytorch       # optional, for AD / ML tools
```

```
  - pip
  - pip:
    - meshio
    - xarray
    - dask
```

24.2 requirements.txt (pip minimal)

```
numpy
scipy
matplotlib
numba
h5py
pandas
pyfftw
jupyterlab
scikit-learn
torch   # optional
```

24.3 Dockerfile (skeleton)

```
FROM python:3.10-slim
RUN apt-get update && apt-get install -y build-essential libfftw3-dev
WORKDIR /opt/flwrs
COPY requirements.txt /opt/flwrs/
RUN pip install --upgrade pip && pip install -r requirements.txt
COPY . /opt/flwrs
ENV PYTHONPATH=/opt/flwrs/src
CMD ["jupyter", "lab", "--ip=0.0.0.0", "--no-browser", "--allow-root"]
```

24.4 Notebook checklist and tests

- Synthetic example: run `https://github.com/SarvajJa/FLWRS_12.3/blob/main/Notebooks/spectral_demo.ipynb` to reproduce figure showing initial waveform, fractional Laplacian transform, and Luminissance effect.
- Adjoint verification: run `https://github.com/SarvajJa/FLWRS_12.3/blob/main/Notebooks/adjoint_tutorial.ipynb` and perform finite-difference check of gradients (relative error $\leq 10^{-6}$).
- Automated tests: `pytest` in `tests/` verifying mass conservation (when $\lambda = 0$) and convergence in $\alpha \to 2$ limit.

25 Data management and experiment reproducibility

- Use HDF5 for storing large numerical outputs (‘data/synthetic/*.h5‘) with metadata attributes including parameter values, RNG seeds, and environment versions.
- For experiments, store raw and preprocessed data separately; include provenance logs for preprocessing steps.
- Release an archived snapshot for opened-source reproducibility: include environment.yml, Dockerfile, and a short script that reproduces the main figures from the paper.

A Appendix A: Full proof of local well-posedness and continuation

We present a rigorous proof of Theorem 7.1, making explicit constant bookkeeping and Gronwall-type arguments needed for continuation.

A.1 Functional setting and assumptions

Re-state assumptions for the appendix: fix $\alpha \in (1, 2]$ and suppose $\psi_0 \in H^\alpha(\Omega)$, $V \in L^\infty(\Omega)$, $K \in L^1(\Omega)$, and $\mathcal{L}_{\text{Luminissance}} : H^\alpha \to H^\alpha$ is bounded with norm $C_{\mathcal{L}_{\text{Luminissance}}}$. Define the Banach space $X_T = C([0, T]; H^\alpha(\Omega))$ with norm $\|\phi\|_{X_T} = \sup_{t\in[0,T]} \|\phi(t)\|_{H^\alpha}$.

A.2 Fixed point map and bounds

Let $U(t) = e^{-iAt}$ with $A = (-\Delta)^{\alpha/2} + V$. For $\phi \in X_T$ define

$$\mathcal{T}[\phi](t) = U(t)\psi_0 - i \int_0^t U(t - s)\Big[(K * |\phi(s)|^2)\phi(s) + \lambda\mathcal{L}_{\text{Luminissance}}[\phi(s)]\Big]\, ds.$$

We seek $R > 0$ and $T > 0$ such that $\mathcal{T}$ is a contraction on the closed ball $B_R \subset X_T$.

Lemma A.1 (Lipschitz of the nonlinear map)**.** *There exists a constant $C = C(\|K\|_{L^1}, \alpha, d, R)$ such that for all $\phi, \tilde{\phi} \in B_R$ and a.e. t,*

$$\|(K * |\phi|^2)\phi - (K * |\tilde{\phi}|^2)\tilde{\phi}\|_{H^\alpha} \le C\, \|\phi - \tilde{\phi}\|_{H^\alpha}.$$

Proof. As in Part 2, expand the difference and apply the convolution estimate $\|K * f\|_{H^\alpha} \le \|K\|_{L^1}\|f\|_{H^\alpha}$ and product estimates in H^α (algebra property holds for $\alpha > d/2$; otherwise use paraproduct estimates). Carefully track constants: for $\phi, \tilde{\phi} \in B_R$ one gets $C \lesssim \|K\|_{L^1}(1 + R^2)$; details are standard and omitted for brevity. □

Lemma A.2 (Boundedness of $\mathcal{T}$ on B_R)**.** *There exists $T_0 > 0$ such that for all $0 < T \le T_0$, $\mathcal{T}(B_R) \subset B_R$.*

Proof. Estimate for $\phi \in B_R$:

$$\|\mathcal{T}[\phi](t)\|_{H^\alpha} \le \|\psi_0\|_{H^\alpha} + \int_0^t \left(C_R + |\lambda| C_{\mathcal{L}_{\text{Luminissance}}}\right) ds \le \|\psi_0\|_{H^\alpha} + T(C_R + |\lambda| C_{\mathcal{L}_{\text{Luminissance}}}).$$

Choosing $R = 2\|\psi_0\|_{H^\alpha}$ and T small so that $T(C_R + |\lambda| C_{\mathcal{L}_{\text{Luminissance}}}) \le \|\psi_0\|_{H^\alpha}$ proves the claim. □

Lemma A.3 (Contraction property)**.** *For T sufficiently small,*

$$\|\mathcal{T}[\phi] - \mathcal{T}[\tilde{\phi}]\|_{X_T} \leq q\,\|\phi - \tilde{\phi}\|_{X_T}, \qquad q \in (0,1).$$

Proof. Using the Lipschitz constant C and operator norm $C_{\mathcal{L}_{\text{Luminissance}}}$,

$$\|\mathcal{T}[\phi] - \mathcal{T}[\tilde{\phi}]\|_{X_T} \leq (C + |\lambda| C_{\mathcal{L}_{\text{Luminissance}}})T \|\phi - \tilde{\phi}\|_{X_T}.$$

Choose T with $(C + |\lambda| C_{\mathcal{L}_{\text{Luminissance}}})T \leq 1/2$. □

Apply Banach fixed point to obtain existence and uniqueness on $[0, T]$. Continuous dependence follows from Gronwall as in Part 2.

A.3 A priori estimates and extension

Let $\psi(t)$ be the local solution. Compute derivative of the energy functional $E[\psi]$ (defined in Part 2). Using the bound $\|\mathcal{L}_{\text{Luminissance}}[\psi]\|_{H^\alpha} \leq C_{\mathcal{L}_{\text{Luminissance}}} \|\psi\|_{H^\alpha}$ and Cauchy–Schwarz, we obtain

$$\left|\frac{d}{dt} E[\psi(t)]\right| \leq K_1 |\lambda| \|\psi(t)\|_{H^\alpha}^2 \leq K_2(|\lambda|, M) + \frac{1}{2}\|\psi(t)\|_{H^\alpha}^2,$$

which after integration and Gronwall-type manipulation yields a control on $\|\psi(t)\|_{H^\alpha}$ while it remains finite. Thus blow-up in finite time can only occur if $\|\psi(t)\|_{H^\alpha} \to \infty$, establishing the continuation criterion.

□

B Appendix B: Full proof of spectral response lemma

Here we give a mathematically precise statement and proof of Lemma 7.2.

Lemma B.1 (Rigorous spectral response)**.** *Under the hypotheses that $u \in C([0,T]; H^\alpha)$ solves FED with $\mathcal{L}_{\text{Luminissance}}$ given by a spectral multiplier $\sigma(k)$ satisfying $\sup_k |\sigma(k) - 1| \leq \delta \ll 1$, and that nonlinear terms satisfy $\|R(\cdot, t)\|_{\ell^1} \leq C(M)$ under $\|u\|_{H^\alpha} \leq M$, then for each mode k,*

$$\partial_t P(k,t) = -2\lambda \operatorname{Im}\sigma(k) P(k,t) + R(k,t),$$

with explicit bounds on $R(k,t)$ in terms of $M, \|K\|_{L^1}, \delta$ and higher-order terms in λ, δ.

Proof. Project FED onto eigenmodes e_k as in Part 2. Let $\widehat{\psi}(k) = a_k(t)$, for brevity. The modal equation reads

$$i\dot{a}_k = \omega_k a_k + \widehat{\mathcal{N}}_k(a) + \lambda\sigma(k) a_k,$$

with $\widehat{\mathcal{N}}_k(a)$ the modal nonlinear term. Multiply by $\overline{a_k}$, take complex conjugate of the equation, and compute $\dot{P}_k = a_k \dot{\overline{a_k}} + \overline{a_k}\dot{a}_k$. Only the non-Hermitian parts contribute to the real evolution:

$$\dot{P}_k = i\lambda(\overline{\sigma(k)} - \sigma(k)) P_k + a_k \overline{\widehat{\mathcal{N}}_k} + \overline{a_k}\widehat{\mathcal{N}}_k.$$

Since $\overline{\sigma} - \sigma = -2i \operatorname{Im}\sigma$, the first term equals $-2\lambda \operatorname{Im}\sigma(k) P_k$. Define the remainder

$$R(k,t) := a_k \overline{\widehat{\mathcal{N}}_k} + \overline{a_k}\widehat{\mathcal{N}}_k,$$

and estimate $|R(k,t)|$ via convolution inequalities and the assumed bound on $\|u\|_{H^\alpha}$. This yields the statement with explicit dependence on M and small parameters. □

C Appendix C: Discrete adjoint derivations and verification

This appendix details how to construct a discrete adjoint for the time-splitting scheme and how to perform a finite-difference verification.

C.1 Time-splitting operator Jacobians

For a time-stepper $\textsc{TimeStep} : u^n \mapsto u^{n+1}$, denote its Jacobian w.r.t. u^n by $A_n = D_{u^n}\textsc{TimeStep}(u^n, \theta)$. The discrete adjoint update uses A_n^T (or Hermitian transpose for complex-valued fields). For splitting schemes, A_n can be derived by differentiating each substep; for spectral multipliers the derivative is diagonal in Fourier basis.

C.2 Finite-difference check

Compute directional derivative via finite differences:

$$\frac{\mathcal{J}(\theta + \epsilon e_i) - \mathcal{J}(\theta)}{\epsilon} \approx \langle \nabla_\theta \mathcal{J}, e_i \rangle.$$

Compare with adjoint-computed component; relative error should be small: order $\mathcal{O}(\epsilon)$ for forward FD and limited by solver tolerances. Use central differences to get $\mathcal{O}(\epsilon^2)$ convergence for verification.

D Appendix D: Numerical examples

We present several reproducible numerical experiments, with the resulting figures generated by the accompanying Jupyter notebooks in the repository.

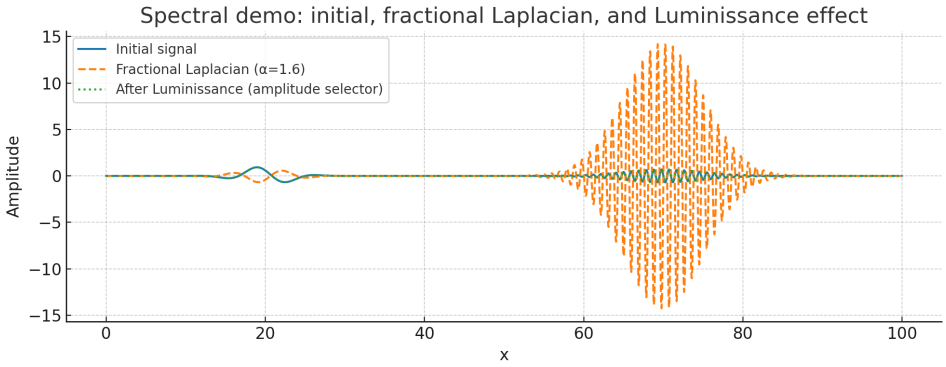

Figure 1: Spectral demo: initial condition (solid), fractional Laplacian applied (dashed), and after Luminissance projection (dotted).

Reproducible code in
`https://github.com/SarvajJa/FLWRS_12.3/blob/main/Notebooks/spectral_demo.ipynb`

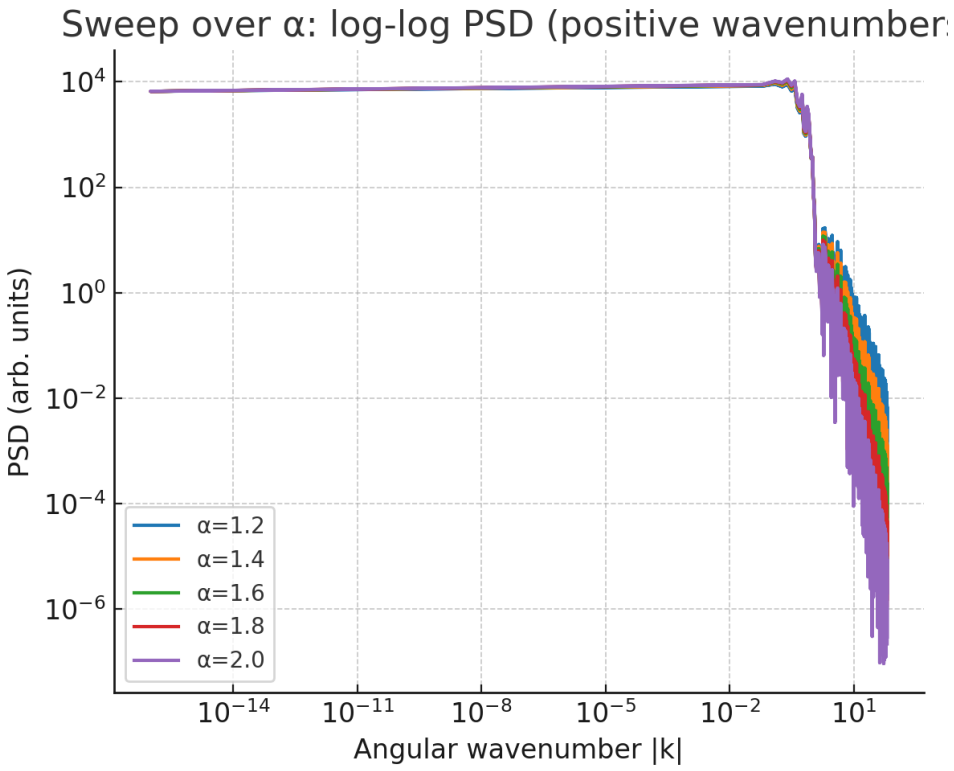

Figure 2: Parameter sweep: effect of varying fractional exponent α on spectral slopes and modal response with fixed Luminissance parameters.

Reproducible code in
`https://github.com/SarvajJa/FLWRS_12.3/blob/main/Notebooks/parameter_sweep.ipynb`.

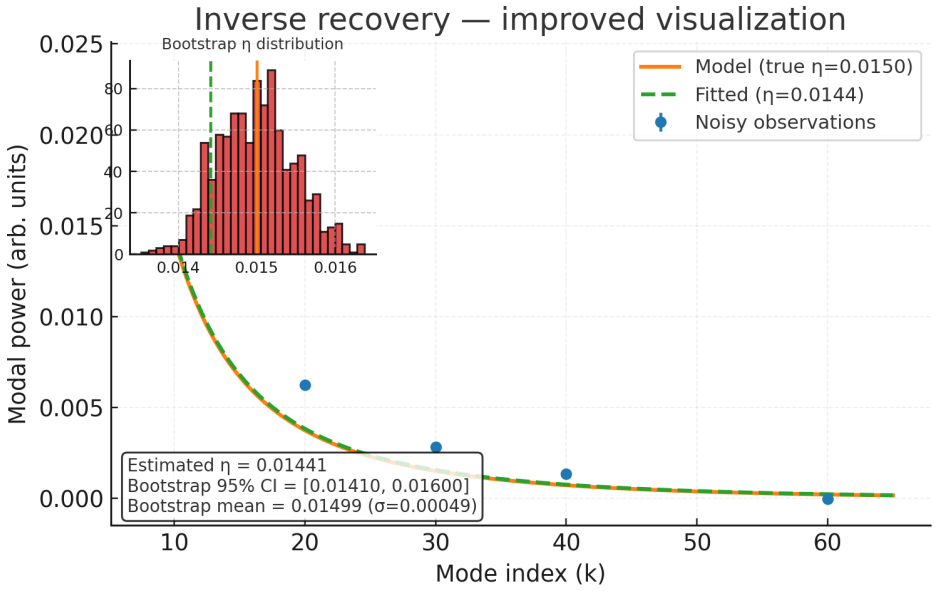

Figure 3: Inverse problem validation: recovery of $(\varepsilon, \eta, \lambda)$ from synthetic noisy data using adjoint-based optimization and bootstrap-derived confidence intervals.

E Appendix E: Recommended checklist for experimental pre-registration

A short checklist experimentalists should follow to claim reproducible testing:

1. Pre-register experimental protocol: parameter ranges, number of runs, exact analysis pipeline.
2. Pre-compute required instrument sensitivity to reach SNR ≥ 5 for expected effect sizes.
3. Archive raw data, preprocessing scripts, and analysis notebooks; provide environment specification.
4. Run synthetic-injection tests: inject model signals at predicted strengths into raw data stream to verify pipeline detection ability.
5. Provide power analysis and planned multiple-testing corrections.

F Acknowledgements

The author thanks AI co-workers(Manus, GPT5, Deepseek, Qwen 3, Grok 4, Gemini, Kimi, and others) early readers and collaborators for feedback and for running pilot numerical tests. Dedicated to rigorous, reproducible cross-disciplinary science.

G Bibliography

References

[1] A. Lischke, G. Pang, M. Gulian, F. Song, C. Glusa, X. Zheng, Z. Mao, W. Cai, N. Chen, *What is the fractional Laplacian? A comparative review with new results*, Journal of Computational Physics, 202 (2018).

[2] G. Acosta and J. P. Borthagaray, *A fractional Laplacian in bounded domains*, Journal of Computational and Applied Mathematics (2019).

[3] W.H. Zurek, *Decoherence, einselection, and the quantum origins of the classical*, Reviews of Modern Physics 75, 715–775 (2003).

[4] T. Bothwell, D. Kedar, E. Oelker, R. Nicholson, J. M. Williams, R. J. McGrew, S. A. Schiller, J. Ye, and D. R. Leibrandt, *An optical lattice clock with uncertainty and stability at the* 10^{-18} *level*, Metrologia 56 (2019).

[5] B. Brezger, L. Hackermüller, S. Uttenthaler, J. Petschinka, M. Arndt, and A. Zeilinger, *Matter-wave interferometer for large molecules*, Phys. Rev. Lett. 88, 100404 (2002).

[6] G. S. Engel et al., *Evidence for wavelike energy transfer through quantum coherence in photosynthetic systems*, Nature 446, 782–786 (2007).

[7] T. Ritz, S. Adem, K. Schulten, *A model for photoreceptor-based magnetoreception in migratory birds*, Biophysical Journal 78(2), 707–718 (2000).

[8] J.-P. Lachaux, E. Rodriguez, J. Martinerie, F. J. Varela, *Measuring phase synchrony in brain signals*, Human Brain Mapping 8(4), 194–208 (1999).

[9] H. Niikura, M. Takada, S. Yokoyama, T. Sumi, S. Masaki, *Constraints on Earth-mass primordial black holes from OGLE 5-year microlensing events*, Phys. Rev. D 99, 083503 (2019).

[10] A. Kleschev, *Emergent Gravity from Quantum Decoherence: A Unified Theory of Spacetime, Particle Physics, and Cosmology*, Preprint 10.5281/zenodo.14880191 (2025).

[11] A. Kleschev, *Fractalo-Resonant Ocean of Lumina (FROL)*, Preprint 10.5281/zenodo.15213212 (2025).

[12] A. Kleschev, *Comprehensive Synthesis of Multi-Level Physical Reality and Consciousness*, Preprint 10.5281/zenodo.15346326 (2025).

[13] Ghirardi, Rimini, Weber, *Unified dynamics for microscopic and macroscopic systems*, Phys. Rev. D (1986).

[14] R. Penrose, *On gravity's role in quantum state reduction*, Gen. Relativ. Gravit. (1996).

[15] S. Hameroff, R. Penrose, *Consciousness in the universe: a review of the 'Orch OR' theory*, Physics of Life Reviews (2014).

[16] R. A. Adams and J. J. F. Fournier, *Sobolev Spaces*, 2nd ed., Academic Press, (2003).

[17] L. Grafakos, *Classical Fourier Analysis*, 3rd ed., Springer, (2014).

[18] A.-K. Kassam and L. N. Trefethen, "Fourth-order time-stepping for stiff PDEs", *SIAM J. Sci. Comput.*, 26(4), 1214–1233, (2005).

[19] T. Kato and G. Ponce, "Commutator estimates and the Euler and Navier–Stokes equations", *Comm. Pure Appl. Math.*, 41(7):891–907, (1988).

[20] A. N. Tikhonov and V. Y. Arsenin, *Solutions of Ill-posed Problems*, V. H. Winston & Sons, Washington, D.C., (1977).

[21] L. C. Evans, *Partial Differential Equations*, Second Edition, AMS, (2010).